CSIRO PUBLISHING

www.publish.csiro.au/journals/rfd *Reproduction, Fertility and Development*, 2009, **21**, 757–772

Molecular cloning and characterisation of heparanase mRNA in the porcine placenta throughout gestation

Jeremy R. Miles[A,B], *Jeffrey L. Vallet*[A], *Brad A. Freking*[A] *and Dan J. Nonneman*[A]

[A]US Department of Agriculture – Agricultural Research Service, Roman L. Hruska US Meat Animal Research Center, Clay Center, NE 68933, USA.

[B]Corresponding author. Email: jeremy.miles@ars.usda.gov

Abstract. Heparanase (HPSE) is an endoglycosidase that specifically degrades heparan sulfate, which is an abundant glycosaminoglycan of the pig placenta. The aims of the present study was to clone cDNA encoding porcine HPSE and characterise the expression level and localisation of *HPSE* mRNA in porcine placentas throughout gestation. Placental tissues were collected from litters on Days 25, 45, 65, 85 and 105 of gestation. Three transcript variants similar to HPSE were identified in the pig placenta. In addition, the *HPSE* gene was mapped to pig chromosome 8 in close proximity to quantitative trait loci for litter size and prenatal survival. Real-time polymerase chain reaction and *in situ* hybridisation were used to characterise the expression of two *HPSE* variants, namely *HPSE v1* and *v2*, in the pig placenta throughout gestation. The expression of *HPSE v1* and *v2* was elevated ($P < 0.01$) in placentas during very early gestation (Day 25) as well as during late gestation (Days 85 and 105). Finally, *HPSE v1* and *v2* mRNA were localised to the cuboidal trophoblast cells of the folded bilayer located nearest to the maternal endometrium. These findings illustrate that HPSE likely plays a role in the development and modification of the pig placenta, which has implications for litter size and prenatal survival.

Additional keywords: extracellular matrix, gene expression, glycosaminoglycans.

Introduction

The placenta provides several critical functions during pregnancy, such as regulating the transport of nutrients, gases and waste, acting as an immunological barrier and serving as a source of various proteins, growth factors and hormones (Regnault *et al*. 2002). As a result, the placenta plays a direct role in regulating fetal growth and survival. In the case of the pig, the regulatory function of the placenta has implications on uterine capacity, litter size and postnatal piglet health (Freking *et al*. 2007; Vallet and Freking 2007). One factor influencing profitability of swine production is sow productivity, which includes litter size at birth and piglet survival to weaning (Zhang *et al*. 2000). Therefore, developing an understanding of the mechanisms that regulate placental function will allow the identification of ways to improve sow productivity.

The efficiency of the placenta is influenced by its overall size, structure and nutrient-specific mechanisms at the fetomaternal interface that facilitate transport between the mother and fetus (Vallet and Freking 2007). The pig placenta is classified as epitheliochorial, consisting of intact epithelium from the endometrium and trophectoderm embedded in a loose stroma. It is characterised by a superficial implantation with no endometrial invasion (Leiser and Kaufmann 1994). The interdigitation of the pig placenta is composed of a folded bilayer in which the ridges of the fetal chorion interdigitate the ridges of the uterine mucosa. These classifications of the pig placenta demonstrate that the pig has one of the least invasive mammalian placentas (Leiser and Kaufmann 1994). To accommodate fetal growth, the fetomaternal interface (i.e. the folded bilayer) of the pig placenta increases in complexity and size as gestation progresses to provide adequate fetomaternal exchange.

The width and complexity of the folds of the bilayer increase during late gestation (gestational Days 85 and 105) compared with early to mid-gestation (Vallet and Freking 2007). In contrast, the placental stromal width external to the folded region decreases during late gestation compared with early to mid-gestation in the pig, suggesting that the development of the folded bilayer occurs at the expense of the placental stroma. Differences in placental morphology during late gestation have also been observed from the smallest and largest fetuses within a litter after unilateral hysterectomy ovariectomy (UHO) of the gilt, which induces intrauterine crowding (Vallet and Freking 2007). The placental stromal widths external to the folded bilayer from the largest fetuses were greater than the smallest fetuses. In contrast, the folded bilayer width and complexity was greater for the smallest fetuses compared with the largest fetuses. These morphometric differences suggest a compensatory mechanism of placentas of small fetuses in a crowded uterine environment, which increases the fetomaternal surface area in response to the overall decreased size of the placentas (Vallet and Freking 2007). Furthermore, these morphometric observations demonstrate that the development of the folded bilayer likely occurs coincident with modification and/or breakdown of the placental stroma.

The pig placenta contains a complex extracellular matrix (ECM) composed of several glycosaminoglycans (GAG; Steele and Froseth 1980). The third most abundant GAG identified in

10.1071/RD09041 1031-3613/09/060757

pig placental homogenates is heparan sulfate (HS) and the level of HS detected in placental homogenates decreases during late gestation (Steele and Froseth 1980). This demonstrates that HS is actively degraded in the pig placenta as pregnancy progresses, which likely modifies its structure. Furthermore, HS has been shown to interact with and sequester many different proteins, cytokines and growth factors within the ECM (Vreys and David 2007; Nasser 2008). As a result, the breakdown of HS results in the local release of various proteins, cytokines and growth factors (Nasser 2008), which likely has additional effects on the development of the placenta.

To date, heparanase-1 (HPSE) is the only endoglycosidase that has been shown to cleave HS side chains specifically (Vreys and David 2007; Nasser 2008). As a result, HPSE has been implicated in several cellular processes, such as tissue morphogenesis (Zcharia *et al*. 2004; Patel *et al*. 2007) and angiogenesis (Vlodavsky *et al*. 2002), and has recently been shown to play a role in mouse (D'Souza *et al*. 2007) and primate (D'Souza *et al*. 2008) embryo implantation and decidualisation. Furthermore, recent evidence in the cow demonstrates that HPSE may play a role in remodelling the cow placenta during pregnancy (Kizaki *et al*. 2003; Hashizume 2007). The human *HPSE* gene is located on chromosome 4 (HSA4; Vlodavsky *et al*. 2002), which is homologous to pig chromosome 8 (SSC8; Rohrer 1999). Several quantitative trait loci (QTL) for female reproductive traits have been identified on SSC8 (Rohrer *et al*. 1999; King *et al*. 2003). Therefore, *HPSE* is a possible candidate gene for association with QTL identified on SSC8, especially those QTL associated with uterine capacity and litter size.

Information pertaining to *HPSE* gene sequence, chromosomal location and mRNA expression in the pig placenta is lacking. Therefore, the aims of the present study were to: (*1*) clone the cDNA encoding pig *HPSE* in the placenta; (*2*) map the chromosomal location of *HPSE* in the pig; (*3*) characterise *HPSE* mRNA expression in the pig placenta throughout gestation; and (*4*) ascertain whether fetal size is associated with *HPSE* expression in placentas throughout gestation. We hypothesised that *HPSE* mRNA will be present in pig placenta and that placental *HPSE* mRNA will be elevated during late gestation, reflecting that HPSE may play a role in modifying the pig placenta during late gestation. Furthermore, we hypothesised that *HPSE* mRNA expression levels in placental tissues will differ between small and large fetuses, consistent with differences in morphometry of the folded bilayer and placental stroma during late gestation.

Materials and methods

Animals

All animal protocols were approved by the US Meat Animal Research Center (USMARC) Animal Care and Use Committee and met the US Department of Agriculture (USDA) guidelines for the care and use of animals. Mention of trade names is necessary to report factually on available data; however, the USDA neither guarantees nor warrants the standard of the product, and the use by the USDA implies no approval of the product to the exclusion of others that may also be suitable. The present study used a subset of randomly selected control line gilts described in Freking *et al*. (2007) and Vallet and Freking (2007). Briefly, gilts underwent UHO surgery at approximately 160 days of age to induce intrauterine crowding during pregnancy (Christenson *et al*. 1987). After 250 days of age, gilts were observed daily for oestrous behaviour. Gilts were naturally mated to randomly selected control line boars at first detection of oestrous and again 24 h later. The initial breeding day was designated as gestational Day 0. Gilts were then randomly assigned to be killed on either Day 25 ($n = 5$), 45 ($n = 5$), 65 ($n = 3$), 85 ($n = 4$) or 105 ($n = 4$) of gestation. At the time of death, the reproductive tract was removed and processed immediately. The broad ligament was trimmed from the uterus and the entire uterus was opened along the antimesometrial surface. Each fetus within the litter was weighed to identify the largest and smallest fetus. For the largest and smallest fetal pig littermates, a section of uterine wall and attached placenta was collected external to the amnion. Sections were placed into plastic cassettes (Sakura Finetak USA, Torrance, CA, USA) and fixed in buffered formalin overnight at room temperature on a rocking platform. A heterogeneous sample of placenta from the largest and smallest fetal pig littermates was also collected, snap-frozen in liquid nitrogen and stored at −80°C until total RNA was extracted.

Processing of uterine/placental sections

Following overnight fixation in buffered formalin, uterine/placental sections were incubated in 70% ethanol overnight at 4°C. The samples were then incubated through a graded series of ethanol (2 h in 95% ethanol, 2 h in absolute ethanol and overnight in absolute ethanol), xylene (2 × 2 h in xylene and overnight in xylene) and paraffin (2 × 2 h paraffin and overnight in paraffin). Tissue samples were then trimmed and embedded in fresh paraffin such that sections of the uterine wall were oriented with the long axis of the uterine horn and were perpendicular to the placental folds. Tissue sections were sectioned serially at 6 μm, placed on coated glass slides and used for *in situ* hybridisation (ISH).

Processing of total RNA and cDNA synthesis

Total RNA from placental tissue was extracted using the RNeasy Mini kit (Qiagen, Valencia, CA, USA) following the manufacturer's instructions. For removal of genomic DNA, DNase-I treatment was performed on the spin column using the DNase provided by the manufacturer (Qiagen). The concentration of RNA was determined using an ND-1000 spectrophotometer (NanoDrop Technologies, Wilmington, DE, USA). There were no differences between samples in the quality and integrity of RNA based on the ratio of absorbance at 260 and 280 nm (approximately 2.0) and visualisation of 28S and 18S rRNA bands in ethidium bromide-stained agarose gels (data not shown). Reverse transcription was performed with 1 μg total RNA isolated from placental tissues using the iScript cDNA synthesis kit (Bio-Rad, Hercules, CA, USA).

Cloning of HPSE cDNA from the pig placenta

Porcine-specific primers (Table 1) were designed using Vector NTI (Invitrogen, Carlsbad, CA, USA) to amplify various coding regions of the pig *HPSE* gene based on expressed

Table 1. Porcine-specific primers used to characterise heparanase mRNA expression in pig placenta throughout gestation

Gene abbreviations used are as specified by the human Gene ID (National Center for Biotechnology Information, http://www.ncbi.nlm.nih.gov/, accessed July 2008) as follows: *HPSE*, heparanase; *GAPDH*, glyceraldehyde-3-phosphate dehydrogenase; *ACTB*, β-actin; *YWHAG*, tyrosine 3-monooxygenase/tryptophan 5-monooxygenase activation protein, gamma; *RPLP2*, ribosomal protein, large P2; *18S*, 18S ribosomal rRNA

Gene ID	Primer	Sequence
HPSE[A]	cDNAF1	5′-GAGATGCTGCTGCGCTG-3′
	cDNAR1	5′-CTGGCAAGGTTTGGTCATTC-3′
	cDNAR2	5′-AATGCAAGCAGCAACTTTGGC-3′
HPSE[B]	Exon8F1	5′-GATGCCACCAAAGAAGATTTTC-3′
	Exon9R1	5′-CTTGTGGGGTCTGGTCTCTTC-3′
GAPDH[C]	RTF	5′-GGCGATGCTGGTGCTACGT-3′
	RTR	5′-CATGGTTCACGCCCATCAC-3′
ACTB	RTF	5′-TCCCTGGAGAAGAGCTACGA-3′
	RTR	5′-TAGAGGTCCTTGCGGATGTC-3′
YWHAG	RTF	5′-GCGAGACCCAGTATGAGAGC-3′
	RTR	5′-AAGGGCCAGGCCTAATCTAA-3′
RPLP2	RTF	5′-GCTGCAGCAGAGGAGAAGAAAGA-3′
	RTR	5′-TTTGCAGGGAGCAGGACTCTAGT-3′
18S	RTF	5′-ATGGCCGTTCTTAGTTGGTG-3′
	RTR	5′-CGCTGAGCCAGTCAGTGTAG-3′
HPSE[D]	RTF*v1*	5′-CAGACCCCACAAGAAGGTGT-3′
	RTR*v1*	5′-GTTCCAGCTCCAAAGAGCAC-3′
HPSE	RTF*v2*	5′-CAGGGCTGAGGACTAAGACG-3′
	RTR*v2*	5′-GAGTGCGAAGCTTTGGAGAG-3′

[A]Of the primers used to amplify the coding region of the *HPSE* gene, cDNAF1/R1 generated partial length coding sequences (CDS) for *HPSE* cDNA and cDNAF1/R2 generated the full-length CDS for *HPSE* cDNA.
[B]Primers used to map chromosomal location of *HPSE* gene in the pig.
[C]Primers used for real-time polymerase chain reaction (PCR) analysis of putative housekeeping genes.
[D]Primers used for real-time PCR and *in situ* hybridisation analysis of *HPSE v1* and *v2*.

sequence tags available through the Dana-Farber Cancer Institute porcine gene index (DFCI ScGI, release 13, 3 July 2008; available from http://compbio.dfci.harvard.edu/tgi/cgi-bin/tgi/gimain.pl?gudb=pig, accessed July 2008; TC314828 and TC319431). Two polymerase chain reactions (PCRs) were performed to amplify partial (HPSE cDNAF1/R1) and full-length (HPSE cDNAF1/R2) coding sequences (CDS) for *HPSE* cDNA. For each PCR, the reaction consisted of 100 ng equivalents of placental cDNA from a large fetus at Day 105 of gestation, 0.4 μM of the appropriate forward and reverse primers, 200 μM dNTPs, 2.5 μL of 10× PCR buffer with 25 mM $MgCl_2$ and 1 U *Taq* polymerase in a 25 μL reaction. Each PCR condition included amplification (95°C for 15 s, 60°C for 15 s and 72°C for 90 s) for 35 cycles, followed by an additional elongation at 72°C for 5 min. Immediately following PCR, amplified products were electrophoresed on a 2% Tris, Borate EDTA (TBE) agarose gel and bands corresponding to the partial (approximately 1500 bp) and full-length (approximately 1600 bp) CDS for *HPSE* cDNAs were excised from the gel and purified using the Gene Clean II kit (MP Biomedicals, Solon, OH, USA) according to the manufacturer's instructions. Partial and full-length CDS *HPSE* clones were generated using the TOPO TA Cloning kit with the pCRII-TOPO vector (Invitrogen) according to the manufacturer's instructions. Positive *HPSE* clones were identified by PCR screening and sequencing. Sequences were aligned with human *HPSE* using Vector NTI (Invitrogen). The predicted protein sequences for pig *HPSE* clones were also determined and aligned with human HPSE using Vector NTI (Invitrogen).

Chromosomal mapping of the pig HPSE *gene*

Chromosomal location of the pig *HPSE* gene was determined using the 90-clone INRA-University of Minnesota porcine radiation hybrid $(IMpRH)_{7000}$ panel (Yerle *et al*. 1998). Porcine-specific primers (Table 1; *HPSE* Exon8F1 and *HPSE* Exon9R1) were designed using Vector NTI (Invitrogen) based on full-length CDS for *HPSE v1* cDNA (Fig. 1) to amplify genomic DNA between exons 8 and 9. The PCR was performed in duplicate reactions, each consisting of 12.5 ng panel DNA, 1.5 mM $MgCl_2$, 200 μM dNTPs, 1 μM each primer, 0.25 U HotStarTaq polymerase (Qiagen) and 1× of the manufacturer buffer in a 15 μL reaction. The PCR conditions consisted of denaturation (94°C for 15 min), followed by amplification (94°C for 20 s, 57°C for 30 s and 72°C for 1.5 min), and then extension at 72°C for 5 min. One-half of each reaction was then run on a 1.5% agarose gel and genotyped manually. The resulting radiation hybrid genotypes were analysed for two- and multipoint linkage with the IMpRH mapping tool and submitted to the IMpRH database (https://www-lgc.toulouse.inra.fr/pig/RH/IMpRH.htm, accessed September 2008). CarthaGene

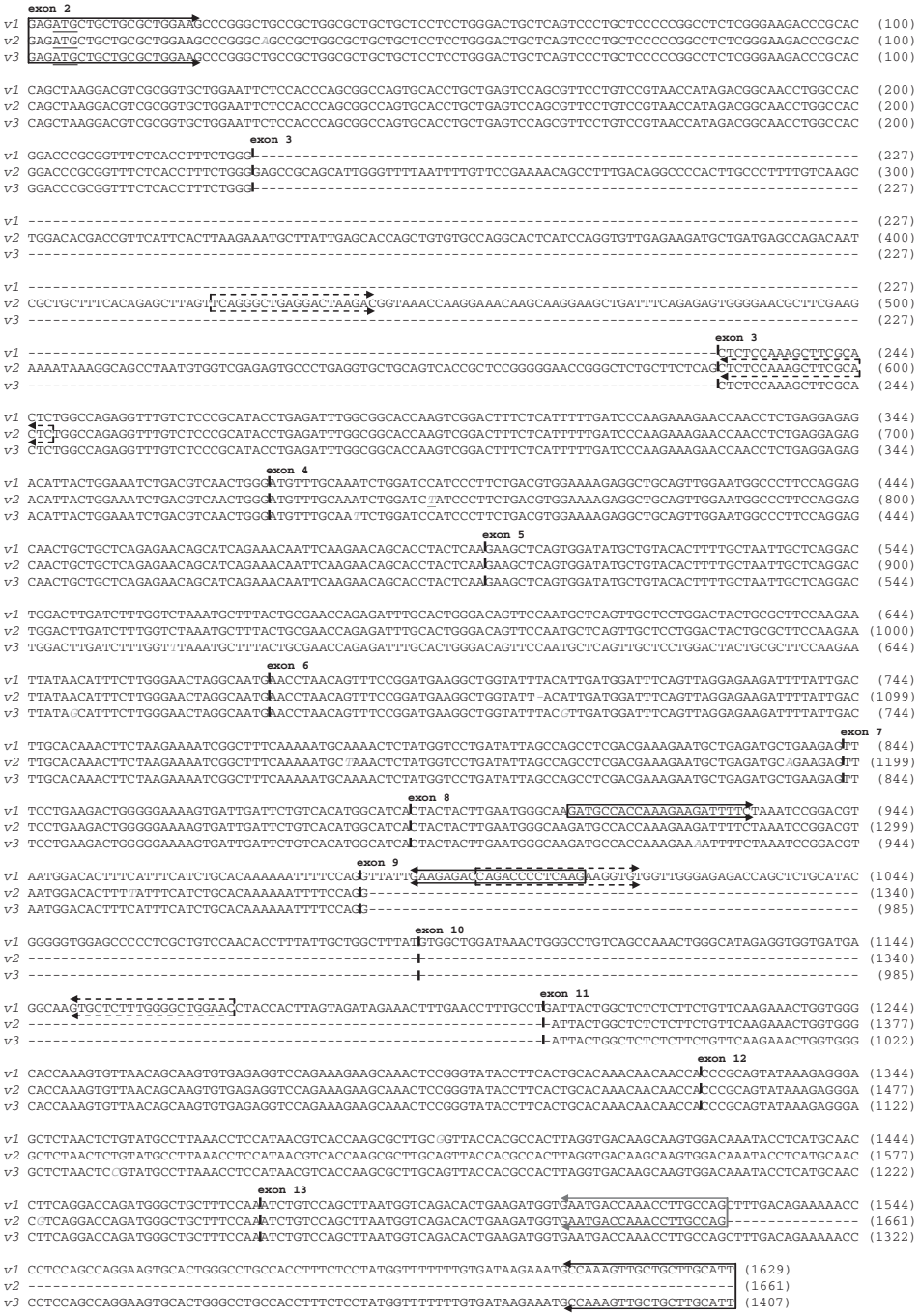

Fig. 1. Nucleotide sequence (5′ to 3′ orientation) of the three porcine heparanase (HPSE) transcript variants (*v1*, *v2* and *v3*) identified in the pig placenta. The underlined nucleotides correspond to the Met start codon for HPSE. Nucleotides that differed between these sequences are italicised and highlighted grey. The 5′ solid black arrows indicate the forward primer (cDNAF1; Table 1) used to generate both partial and full-length coding sequence (CDS) cDNAs, whereas the 3′ solid grey arrows indicate the reverse primer (cDNAR1; Table 1) used to generate the partial length CDS cDNAs and the 3′ solid black arrows indicate the reverse primer (cDNAR2; Table 1) used to generate the full-length CDS cDNAs. The solid black arrows over *v1* designate the forward (Exon8F1; Table 1) and reverse (Exon9R1; Table 1) primers used to amplify genomic DNA for radiation hybrid mapping of the *HPSE* gene. The dashed black arrows over *v1* designate the forward (RTFv1; Table 1) and reverse (RTRv1; Table 1) primers specifically used to measure *HPSE v1* by real-time polymerase chain reaction (PCR) and *in situ* hybridisation (ISH). The dashed black arrows over *v2* designate the forward (RTFv2; Table 1) and reverse (RTRv2; Table 1) primers specifically used to measure *HPSE v2* by real-time PCR and ISH. The vertical dashed lines indicate the predicted exon boundaries and corresponding exon number in the pig sequence based on the exon boundaries identified in the human (Dong *et al*. 2000). The nucleotide sequences for these variants have been submitted to GenBank (http://www.ncbi.nlm.nih.gov/Genbank/index.html, accessed March 2009) under the accession numbers FJ713408, FJ713409 and FJ713410.

Table 2. Gestational day effects on the expression of putative housekeeping genes in pig placenta throughout gestation

Data were log transformed before analysis and back-transformed to observed values. Values are reported as least-squares means, with values in parentheses indicating the range of error within 1 s.e.m. after back-transformation. Transcript expression was measured using the linear Ct value (2^{-Ct}). Values within rows with different superscript letters differ significantly. Gene abbreviations used are as specified by the human Gene ID (National Center for Biotechnology Information, http://www.ncbi.nlm.nih.gov/, accessed July 2008) as follows: *GAPDH*, glyceraldehyde-3-phosphate dehydrogenase; *ACTB*, β-actin; *YWHAG*, tyrosine 3-monooxygenase/tryptophan 5-monooxygenase activation protein, gamma; *RPLP2*, ribosomal protein, large P2; *18S*, 18S ribosomal rRNA

Gene ID	Day of gestation					*P* value
	25	45	65	85	105	
GAPDH	0.78[a] (0.66–0.92)	0.37[b] (0.44–0.31)	0.41[b] (0.33–0.51)	0.13[c] (0.11–0.16)	0.13[c] (0.10–0.15)	<0.001
ACTB	0.66[a] (0.56–0.78)	0.38[b] (0.32–0.44)	0.29[b] (0.23–0.35)	0.10[c] (0.08–0.12)	0.08[c] (0.07–0.10)	<0.001
YWHAG	0.44[a] (0.36–0.53)	0.38[a] (0.31–0.46)	0.29[a] (0.22–0.37)	0.13[b] (0.11–0.17)	0.15[b] (0.12–0.19)	<0.01
RPLP2	0.77[a] (0.67–0.88)	0.41[b] (0.36–0.47)	0.42[b] (0.35–0.50)	0.17[c] (0.14–0.19)	0.12[c] (0.11–0.15)	<0.001
18S	0.64[a] (0.48–0.86)	0.34[ab] (0.25–0.46)	0.44[a] (0.30–0.64)	0.20[b] (0.14–0.28)	0.17[b] (0.12–0.24)	0.05

(http://www.inra.fr/internet/Departements/MIA/T//CartaGene/, accessed September 2008) was used to estimate the multipoint marker distance and the marker position was estimated from microsatellite positions on the USMARC linkage map (http://www.marc.usda.gov/genome/swine/swine.html, accessed September 2008).

Cloning of HPSE v1 *and* v2 *cDNA for real-time PCR and ISH analysis*

Porcine-specific primers (Table 1) were designed using Primer3 software (Rozen and Skaletsky 2000) based on partial length CDS *HPSE v1* and *v2* cDNA sequences (Fig. 1). Each PCR consisted of 100 ng equivalents of placental cDNA from a large fetus at Day 105 of gestation, 0.4 μM of the appropriate forward and reverse primers, 200 μM dNTPs, 2.5 μL of 10× PCR buffer with 2.5 mM $MgCl_2$, and 1 U *Taq* polymerase in a 25 μL reaction. Each PCR condition included amplification (95°C for 15 s, 60°C for 15 s and 70°C for 45 s) for 40 cycles, followed by an additional elongation at 72°C for 5 min. Immediately following PCR, resulting PCR products for the *HPSE v1* (171 bp) and *v2* (180 bp) were electrophoresed in a 2% TBE agarose gel and desired bands were excised from the gel and purified using the Gene Clean II kit (MP Biomedicals) according to the manufacturer's instructions. Fragments of *HPSE v1* and *v2* were cloned using the TOPO TA Cloning kit with the pCR4-TOPO vector (Invitrogen) according to the manufacturer's instructions. Positive clones for each variant were identified by PCR screening and the orientation of each clone was determined by sequence analysis. Plasmids were isolated from *HPSE v1*- or *v2*-positive clones using the Maxi-prep kit (Qiagen) according to the manufacturer's instructions. The isolated plasmid (50 μg) of each variant was linearised with *Not*I (Promega, Madison, WI, USA) or *Spe*I (Promega) overnight at 37°C. The linearised plasmid for each variant was electrophoresed in a 1% TBE agarose gel to confirm a single, linearised plasmid, which was excised from the gel and purified using the Gene Clean II kit (MP Biomedicals) according to the manufacturer's instructions. The linearised plasmid for each variant was stored at −20°C until used for real-time PCR and ISH analysis of *HPSE v1* and *v2*.

Real-time PCR analysis of transcript expression levels in the pig placenta

Porcine-specific primers (Table 1) for *GAPDH*, *ACTB*, *YWHAG*, *RPLP2* and *18S* were used to analyse internal reference control transcripts using real-time PCR. A two-step, real-time PCR method was used for transcript expression analysis in which real-time PCR was performed with the Chromo4 real-time PCR detection system (Bio-Rad). Each real-time PCR was assayed in duplicate and consisted of 25 ng equivalents of cDNA, 0.2 μM of the appropriate forward and reverse primer and 12.5 μL of 1× iTaq SYBR Green Supermix with ROX (Bio-Rad) in a 25 μL reaction. All PCR conditions included denaturation (95°C for 2 min) followed by amplification (95°C for 15 s, 60°C for 15 s and 70°C for 45 s) for 40 cycles. Melting curve analysis and gel electrophoresis were used to confirm amplification of a single product of the predicted size. The PCR product from a representative sample of PCR for each transcript was verified by sequence analysis to confirm amplification of the correct cDNA. Expression levels for each transcript were based on the threshold cycle (Ct) values determined using Opticon Monitor 3 software (Bio-Rad). For each transcript, one assay was performed containing all the samples, with intraassay CVs of 8.8%, 8.6%, 4.9%, 7.0% and 4.5% for *GAPDH*, *ACTB*, *YWHAG*, *RPLP2* and *18S*, respectively, after converting the exponential Ct to the linear Ct using the formula 2^{-Ct} (Livak and Schmittgen 2001). Preliminary analysis of the relative expression level based on the linearised Ct value (2^{-Ct}; Livak and Schmittgen 2001) for all putative housekeeping genes (*GAPDH*, *ACTB*, *YWHAG*, *RPLP2* and *18S*) indicated that each differed among days of gestation (Table 2) and between fetal littermate size (Table 3). Therefore, an absolute standard curve method (Pfaffl 2004) was used to determine the level of *HPSE v1* and *v2* mRNA in the pig placenta.

The cRNA for absolute standard curves was synthesised by *in vitro* transcription of the *HPSE v1* and *v2* cDNAs using the MAXIscript kit (Ambion, Austin, TX, USA) according to the manufacturer's instructions. The *Spe*I linearised plasmids for each variant were used to transcribe sense cRNA, which was subsequently reverse transcribed to cDNA. The concentration of sense cRNA was determined using a ND-1000 spectrophotometer (NanoDrop Technologies) and reverse transcription was

Table 3. Effect of littermate fetal size on the expression of putative housekeeping genes in pig placenta throughout gestation

Data were log transformed before analysis and back-transformed to observed values. Values are reported as least-squares means, with values in parentheses indicating the range of error within 1 s.e.m. after back-transformation. Transcript expression was measured using the linear Ct value (2^{-Ct}). Gene abbreviations used are as specified by the human Gene ID (National Center for Biotechnology Information, http://www.ncbi.nlm.nih.gov/, accessed July 2008) as follows: *GAPDH*, glyceraldehyde-3-phosphate dehydrogenase; *ACTB*, β-actin; *YWHAG*, tyrosine 3-monooxygenase/tryptophan 5-monooxygenase activation protein, gamma; *RPLP2*, ribosomal protein, large P2; *18S*, 18S ribosomal rRNA

Gene ID[A]	Fetal size		*P* value
	Small	Large	
GAPDH	0.35 (0.31–0.40)	0.23 (0.21–0.26)	0.02
ACTB	0.28 (0.25–0.32)	0.18 (0.16–0.20)	0.01
YWHAG	0.30 (0.26–0.34)	0.21 (0.18–0.24)	0.08
RPLP2	0.35 (0.32–0.39)	0.27 (0.24–0.29)	0.05
18S	0.35 (0.29–0.42)	0.29 (0.24–0.35)	0.38

performed with 1 ng amplified sense cRNA for each variant using the iScript cDNA synthesis kit (Bio-Rad). Real-time PCR assays were performed under similar conditions as described for the putative housekeeping genes to determine the level of *HPSE v1* and *v2*. In addition, a fourfold serial dilution of cDNA (ranging from 200 to 0.78 fg equivalents cDNA) from the amplified sense cRNA was included in the PCR assay for each respective transcript. The intraassay CVs for *HPSE v1* and *v2* were 6.1% and 13.7%, respectively, after converting to the linearised Ct values. To determine levels of *HPSE v1* and *v2*, sample Ct values were plotted against the regression equation generated for each absolute standard curve, as follows:

$$HPSE\ v1 = (\text{sample Ct} - 29.741)/-3.6667$$
$$HPSE\ v2 = (\text{sample Ct} - 29.64)/-3.4627$$

Values are expressed as copy number per 25 ng total RNA. The slope of the regression line generated from each serial dilution was used to calculate the PCR amplification efficiency as follows:

$$E = 10^{(-1/\text{slope})}$$

where E = 1.87 and 1.94, for *HPSE v1* and *v2*, respectively (Pfaffl 2001). To compare the relationship between *HPSE v1* and *v2* expression within individual placentas, the linearised Ct values based on the PCR amplification efficiency (E^{-Ct}) for each variant were compared taking into account differences in the PCR amplification efficiency for each primer set (Pfaffl 2001).

In situ *hybridisation analysis of* HPSE v1 *and* v2 *mRNA localisation in the pig placenta*

Radiolabelled antisense or sense cRNA probes for *HPSE v1* and *v2* were transcribed *in vitro* using the MAXIscript kit (Ambion) according to the manufacturer's instructions. Antisense probes for both variants were generated using *Not*I linearised plasmids, T3 RNA polymerase and [^{35}S]-uridine 5′-triphosphate (UTP; specific activity 4.625×10^{13} Bq mmol^{-1}; Perkin Elmer, Boston, MA, USA). Sense probes for both variants were generated using *Spe*I linearised plasmids, T7 RNA polymerase and [^{35}S]-UTP. Localisation of *HPSE v1* and *v2* mRNA in uterine/placental tissue sections was performed using a modified *in situ* hybridisation method (Spencer *et al*. 1995). Briefly, uterine/placental tissue sections from representative large fetal littermates at Days 25, 45, 65, 85 and 105 of gestation ($n = 3$ representatives per day) were deparaffinised in xylene and rehydrated through a graded series of ethanol. All washing and hybridisation protocols were performed in a similar manner as reported by Spencer *et al*. (1995), except that sections were washed with a 0.1 M triethanolamine/0.25% acetic anhydride (Sigma, St Louis, MO, USA) solution for 5 min at room temperature before prehybridisation. Antisense and sense cRNA probes for both variants were diluted in hybridisation buffer at 10 000 d.p.m. μL^{-1} and 100 μL hybridisation buffer containing the appropriate probe was placed on representative tissue sections. Prior to post-hybridisation dehydration, tissue sections were stained for 15 s with 0.22 μM filtered haematoxylin (Sigma). Following dehydration, slides were dipped in liquid Kodak autoradiography emulsion (Kodak, Rochester, NY, USA), allowed to dry and stored with desiccant in a light tight box for 2 weeks at 4°C. Slides were then developed for 2 min in Dektol developer (Kodak) diluted 1 : 1 in distilled water, rinsed in distilled water for 1 min and fixed in fixer (Kodak) for 5 min. Tissue sections were dehydrated through a graded series of ethanol to xylene and mounted with Permount (Sigma). Brightfield and darkfield photomicrographs of tissue sections were illuminated using an Axioplan2 microscope (Zeiss, New York, NY, USA). Photomicrographs were taken using an Optronics DEI 750 camera (Optronics, Goleta, CA, USA) and images were processed using the Bioquant Nova image analysis software (Bioquant, Nashville, TN, USA).

Statistical analysis

Prior to statistical analysis, transcript expression data were log transformed to normalise the data and then back-transformed

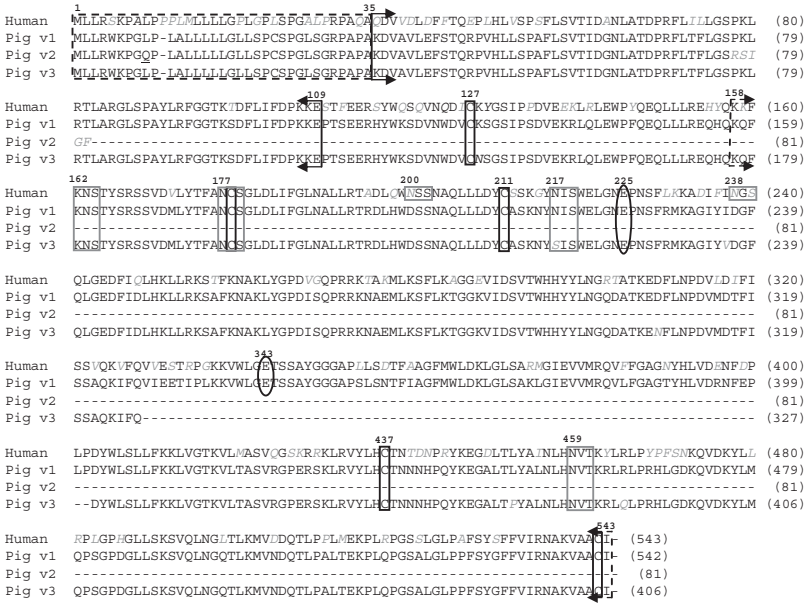

Fig. 2. Alignment of human heparanase (HPSE; Vlodavsky *et al*. 1999) with the predicted amino acid sequences of the three porcine *HPSE* transcript variants identified in the pig placenta. Amino acid residues that differed between these sequences are italicised and highlighted grey. The dashed black box illustrates a potential N-terminal signal sequence. The solid black arrows correspond to the 8-kDa subunit and the dashed black arrows correspond to the 50-kDa subunit identified in the human. The solid black boxes highlight the Cys residues. The solid grey boxes indicate N-linked glycosylation sites and the solid black ovals illustrate the two catalytic Glu residues, a proton donor at Glu^{225} and a nucleophile at Glu^{343} (Vreys and David 2007).

for reporting values. All data were analysed using the MIXED model procedure for analysis of variance (ANOVA; Steel *et al*. 1997; SAS 2003) and results are reported as the least-squares mean ± s.e.m. The model used for the analysis of transcript expression levels included the fixed effects of day of gestation, fetal size (i.e. small *v.* large) and their interaction with the random effect of gilt within day of gestation. When a significant *F* statistic ($P < 0.05$) was obtained, means were separated using a series of orthogonal contrasts (SAS 2003). The orthogonal contrasts for the putative housekeeping transcript expression levels included comparisons between Days 45 and 65, Days 85 and 105, the average of Days 45 and 65 *v.* the average of Days 85 and 105, and Day 25 *v.* the average of Days 45, 65, 85 and 105. The orthogonal contrasts for *HPSE v1* and *v2* expression levels included comparisons between Days 45 and 65, Days 85 and 105, Days 25 *v.* the average of Days 85 and 105, and the average of Days 25, 85, and 105 *v.* Days 45 and 65. The relationship between *HPSE v1* and *v2* expression levels within individual placentas was further assessed by regression analysis (Steel *et al*. 1997; SAS 2003).

Results

Cloning of HPSE *cDNA from the pig placenta*

The amplification and cloning of cDNA using *HPSE* cDNAF1 and *HPSE* cDNAR1 primers (Fig. 1; Table 1) identified two partial length CDS cDNAs similar to human HPSE. The more abundant *HPSE* variant (*HPSE v1*) was identified in six of the seven initial clones screened. The *HPSE v1* variant consisted of a 1528-bp cDNA sequence that included most of the protein coding region corresponding to a predicted protein of 508 amino acids that shares 80% identity with human HPSE (Vlodavsky *et al*. 1999). An additional *HPSE* variant (*HPSE v2*) was also obtained in one of the seven initially screened clones. The *HPSE v2* variant consisted of a 1661-bp cDNA sequence that contained an additional 355 bp in sequence relative to *HPSE v1* at nucleotide 244 (Fig. 1) and human *HPSE* mRNA (Vlodavsky *et al*. 1999), which introduced several stop codons and resulted in a predicted truncated protein of 81 amino acids (Fig. 2). This variant also included a 222 bp deletion in the sequence relative to *HPSE v1* between nucleotides 985 and 1207 (Fig. 1). These sequence differences were exploited to distinguish between *HPSE v1* and *v2* using real-time PCR. An additional reverse primer (*HPSE* cDNAR2; Fig. 1) in conjunction with the original forward primer (*HPSE* cDNAF1; Fig. 1) was used to obtain the remainder of the CDS for *HPSE*. Again, two variants corresponding to HPSE were identified. The most abundant variant (in 10 of 13 clones) was identical to *HPSE v1*, consisting of a 1629 bp cDNA sequence (Fig. 1) that corresponded to a predicted protein of 542 amino acids (Fig. 2) and sharing 80% homology with the human HPSE (Vlodavsky *et al*. 1999). Interestingly, *HPSE v2* was not identified from the full-length CDS clones, suggesting that this variant may differ in 3′ sequence compared with the

HPSE v1. However, a third variant (*HPSE v3*) was obtained from the remaining three clones. The *HPSE v3* cDNA was identical to *HPSE v1* except for the presence of the 222 bp deletion observed in *HPSE v2*, which resulted in a sequence of 1407 bp (Fig. 1) and a predicted protein of 468 amino acids (Fig. 2). Based on the human *HPSE* exon boundaries (Dong *et al*. 2000) illustrated in Fig. 1, the coding region of the pig *HPSE* gene consisted of 12 exons (exons 2–13). The sequences corresponding to porcine *HPSE v1*, *v2* and *v3* mRNA have been submitted to GenBank (http://www.ncbi.nlm.nih.gov/Genbank/index.html, accessed March 2009) under the accession numbers FJ713408, FJ713409 and FJ713410, respectively.

The predicted pig HPSE proteins from the three identified *HPSE* mRNA variants were aligned with the human HPSE protein (Fig. 2; Vlodavsky *et al*. 1999). Human HPSE contains an N-terminal signal sequence (Fig. 2) that appears to be conserved in all three predicted pig proteins. There are five Cys residues (Fig. 2) in human HPSE, all of which are conserved in the predicted proteins for *HPSE v1* and *v3*. Human HPSE contains six N-linked glycosylation sites (Fig. 2) and four of these sites are conserved in pig proteins for *HPSE v1* and *v3*; however, glycosylation sites at Asn^{200} and Asn^{238} are missing in the pig proteins. Active human HPSE forms a heterodimer that consists of a 50-kDa subunit that non-covalently associates with an 8-kDa subunit (Fig. 2; Vreys and David 2007); these sequences appear to be conserved in the pig protein for *HPSE v1*. Interestingly, the predicted pig protein for *HPSE v2* only includes part of the 8-kDa subunit, whereas the pig protein for *HPSE v3* is missing 74 amino acids in the 50-kDa subunits. Finally, the two critical residues necessary for the hydrolysis of HS chains, a proton donor at Glu^{225} and a nucleophile at Glu^{343} (Fig. 2; Hulett *et al*. 2000; Vreys and David 2007), are conserved between human HPSE and the protein coded by *HPSE v1*. Taken together, the conservation of the predicted pig protein for *HPSE v1* with human HPSE suggests that the pig placenta produces a functional HPSE protein.

Chromosomal mapping of the HPSE *gene*

Chromosomal location of the pig *HPSE* gene was determined using the porcine radiation hybrid $(IMpRH)_{7000}$ panel (Yerle *et al*. 1998). Using the IMpRH mapping tool (http://www.toulouse.inra.fr/lgc/pig/RH/IMpRH.htm, accessed September 2008), the pig *HPSE* gene was localised on SSC8 between markers CL390254 and CL414431 with logarithm of odds (LOD) scores of 15.02 and 9.02, respectively. In addition, the CarthaGene RH software (http://www.inra.fr/internet/Departements/MIA/T//CarthaGene/, accessed September 2008) demonstrated that the pig *HPSE* gene mapped in close proximity to marker CL390254 (LOD score of 14.2) on SSC8. Based on the integrated porcine radiation hybrid and linkage map (Meyers *et al*. 2005), the pig *HPSE* gene is located between 126.1 and 127.7 cM on SSC8 (based on SW1980 and S0178 marker positions, respectively; http://www.marc.usda.gov/genome/swine/swine.html, accessed September 2008). The positions of the markers CL390254 and CL414431 correspond to 85.11 and 83.66 Mb on HSA4, respectively (Meyers *et al*. 2005), which is consistent with the location of human *HPSE* at 84.43 Mb on HSA4 (*Homo sapiens* Genome Build 36.3; http://www.ncbi.nlm.nih.gov/, accessed March 2009).

Transcript expression levels in the pig placenta

No significant fetal size × gestational day interactions were observed for the expression of *GAPDH* ($P = 0.67$), *ACTB* ($P = 0.66$), *YWHAG* ($P = 0.85$), *RPLP2* ($P = 0.61$) or *18S* ($P = 0.31$). However, the expression levels of all putative housekeeping genes were different between gestational days, with the greatest expression observed in early gestation placentas (Day 25) compared with late gestation placentas (Days 85 and 105); mid-gestation placentas (Days 45 and 65) displayed an intermediate level of expression (Table 2). Furthermore, the expression of *GAPDH*, *ACTB* and *RPLP2* was significantly increased in placentas from small fetal littermates compared with placentas from large fetal littermates (Table 3). A similar tendency was observed for the expression of *YWHAG* in placentas from small fetal pig littermates. Because both gestational day and fetal size differences were observed for these putative housekeeping genes, these transcripts would not serve as an appropriate internal controls to normalise target gene expression for relative quantification. As a result, an absolute standard curve method (Pfaffl 2004) was used to determine expression levels for *HPSE v1* and *v2* mRNA in pig placenta.

No significant fetal size × gestational day interactions were observed for the expression of *HPSE v1* or *v2*. In addition, there were no significant fetal size differences observed for the expression of *HPSE v1* or *v2*. However, a significant gestational day effect for the expression of *HPSE v1* was detected in pig placentas (Fig. 3). The expression of *HPSE v1* was not significantly different between placentas at Days 25, 85 and 105 of gestation. In contrast, the expression of *HPSE v1* was decreased ($P < 0.01$) in mid-gestation placentas (Days 45 and 65) compared with early (Day 25) and late (Days 85 and 105) gestation placentas. Similarly, a significant gestational day effect for the expression of *HPSE v2* was detected in pig placentas (Fig. 4). The expression

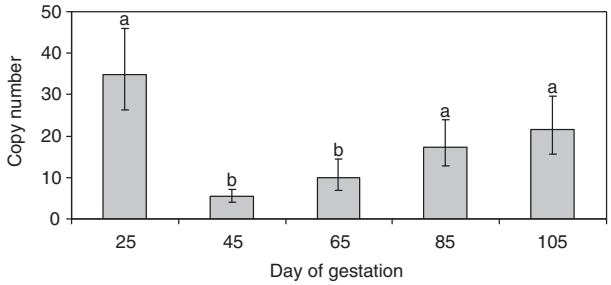

Fig. 3. Expression levels of *HPSE v1* mRNA measured by real-time polymerase chain reaction in pig placenta throughout gestation. Data were log transformed before analysis and back-transformed to observed values. Least-squares mean ± s.e.m. values are expressed as copy number per 25 ng total RNA. Statistical analysis demonstrated that only gestational day has a significant effect ($P < 0.01$) on the expression level of *HPSE v1* in the pig placenta. Copy numbers with different superscripts are significantly different ($P < 0.01$).

of *HPSE v2* did not differ between early (Day 25) and late (Days 85 and 105) gestation placentas. In contrast, the expression of *HPSE v2* was decreased ($P < 0.01$) in mid-gestation placentas (Days 45 and 65) compared with early (Day 25) and late (Days 85 and 105) gestation placentas. Figure 5 shows the relationship between the mRNA expression levels of *HPSE v1* and *v2* within individual pig placentas. There was a significant positive linear relationship between the expression of *HPSE v1* and *v2* with a correlation of 0.63. This indicated that the expression of *HPSE v1* is positively correlated with *HPSE v2* within individual placentas. Furthermore, the slope of the regression analysis illustrates that the *HPSE v1* expression level was 22.6-fold greater than *HPSE v2*, demonstrating that *HPSE v2* is a rarer transcript variant compared with *HPSE v1*.

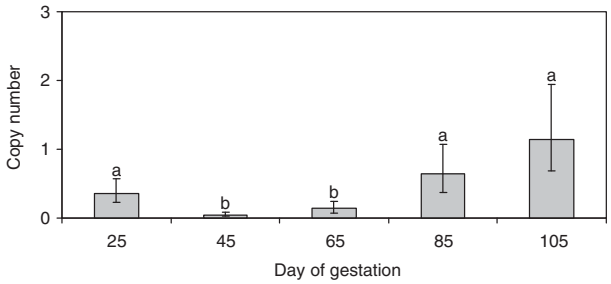

Fig. 4. Expression levels of *HPSE v2* mRNA measured by real-time polymerase chain reaction in pig placenta throughout gestation. Data were log transformed before analysis and back-transformed to observed values. Least-squares mean ± s.e.m. values are expressed as copy number per 25 ng total RNA. Statistical analysis demonstrated that only gestational day has a significant effect ($P < 0.01$) on the expression level of *HPSE v2* in the pig placenta. Copy numbers with different superscripts are significantly different ($P < 0.01$).

HPSE v1 *and* v2 *mRNA localisation in the pig placenta*

Figure 6 shows the mRNA localisation of *HPSE v1* in the pig placenta throughout gestation. Owing to the poor attachment of the trophectoderm and uterine endometrium at Day 25 of gestation, only localised regions of the trophectoderm were attached to the uterine epithelium in Day 25 uterine/placental sections. Within these localised areas of attachment, *HPSE v1* signal was identified in the epithelial bilayer with the majority of the signal localised to the trophectoderm. Furthermore, the epithelial bilayer had only minimal folding at Day 25 of gestation. By Day 45 of gestation, the trophectoderm and uterine epithelium were firmly attached and the folding of the epithelial bilayer was apparent, although the width and complexity of the folds were minimal. The signal for *HPSE v1* still appeared to be localised within the epithelial bilayer at Day 45; however, the signal was reduced significantly, making it difficult to determine which cells were positive for *HPSE v1*. At Day 65 of gestation, the complexity of the folded bilayer had started to increase, as observed by the initiation of secondary branching, although the width of the folded bilayer remained similar to Day-45 placentas. The signal of *HPSE v1* was also increased by Day 65 compared with Day 45, with the majority of the signal being localised to trophoblast cells within the folds nearest the endometrium. By Days 85 and 105 of gestation, not only was the complexity of the folded bilayer increased, but the width of the folds of the bilayer was also increased relative to earlier stages of gestation. The signal of *HPSE v1* had increased markedly during late gestation in the folded bilayer and, again, the majority of the signal was localised to cuboidal trophoblast cells within the folds closest to

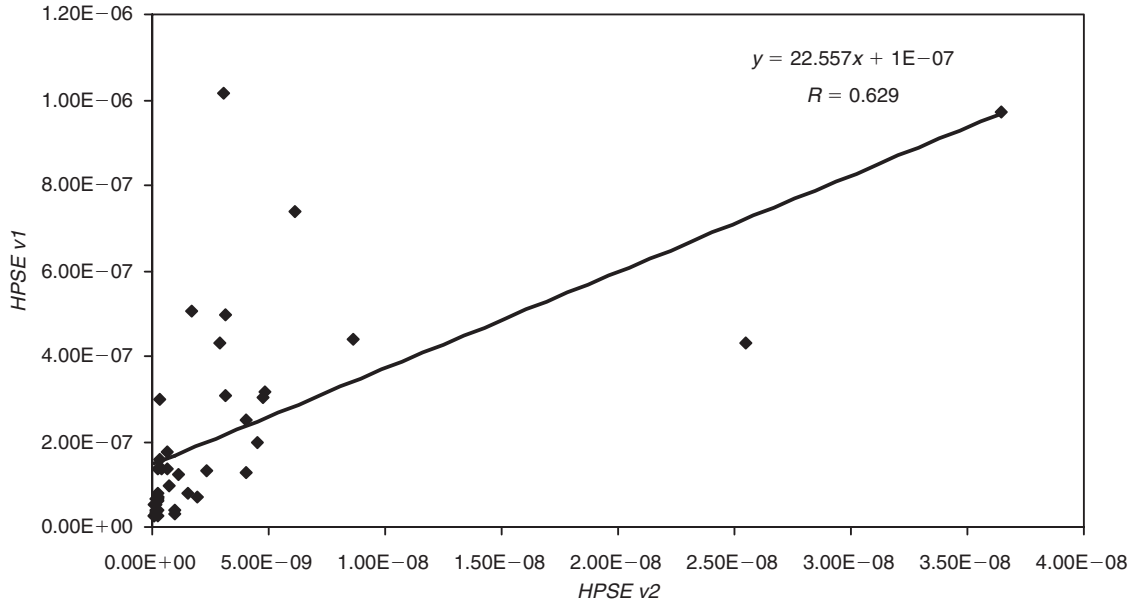

Fig. 5. Relationship between the mRNA expression levels of *HPSE v1* and *v2* in individual pig placentas.

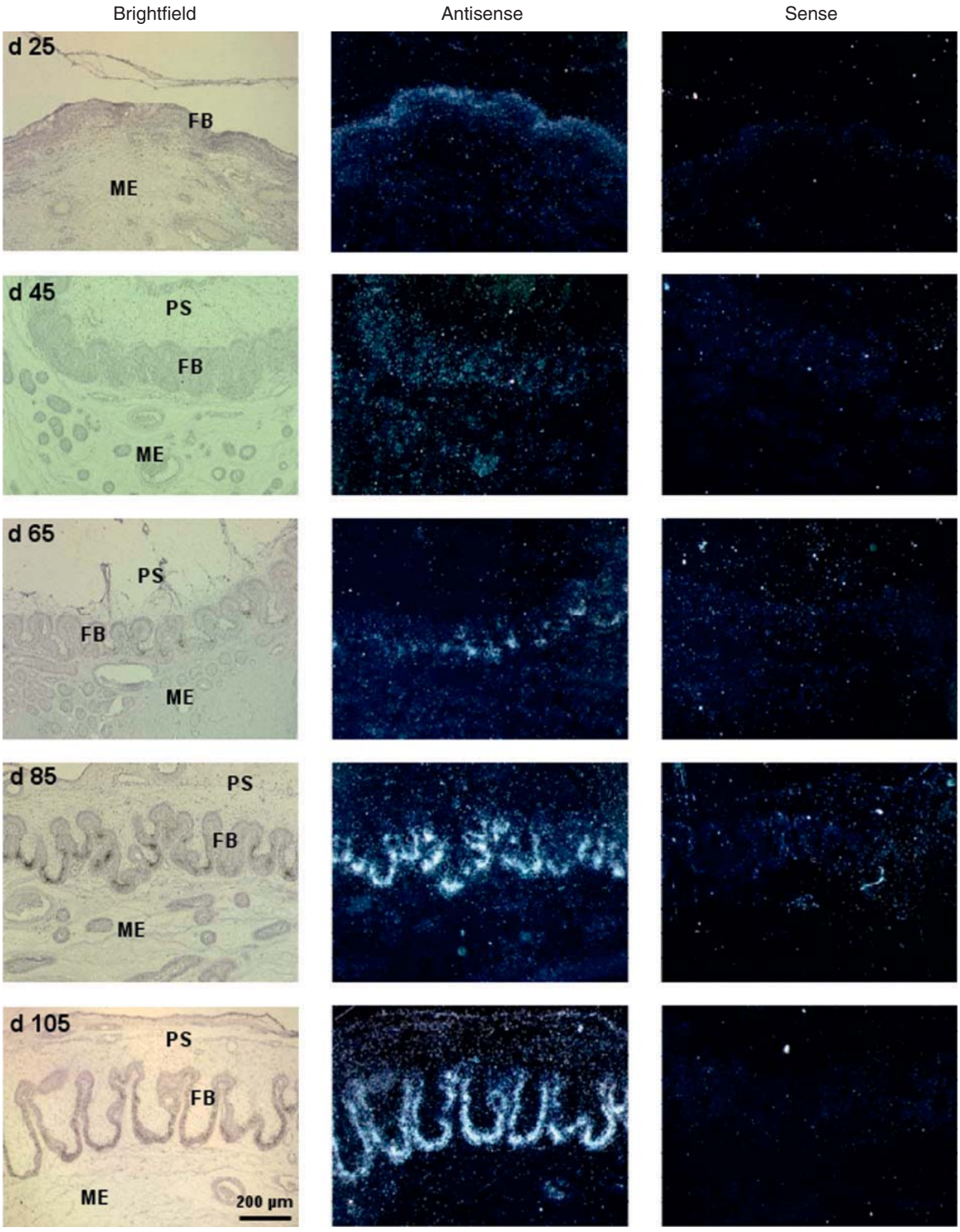

Fig. 6. *In situ* hybridisation analysis of *HPSE v1* mRNA localised to the fetomaternal interface of the pig placenta throughout gestation. Corresponding brightfield and darkfield with antisense probe or darkfield with sense probe photomicrographs are presented from uterine/placental cross-sections at Days 25, 45, 65, 85 and 105 of gestation. Note that throughout gestation the *HPSE v1* signal is localised to the trophectoderm of the folded bilayer (FB) and is lacking in cells of the maternal endometrium (ME) or placental stroma (PS). Scale bar = 200 μm.

the endometrium. Furthermore, *HPSE v1* signal was lacking in cells of the myometrium (data not shown), uterine glands, uterine blood vessels, placental stroma, placental vessels and placental areoli (Fig. 7) throughout gestation.

Figure 8 shows the mRNA localisation of *HPSE v2* in the pig placenta throughout gestation. During early to mid-stages of gestation (Days 25, 65 and 85), very limited signal for *HPSE v2* was localised to the folded bilayer. By late gestation (Days 85 and 105), *HPSE v2* signal was increased and was primarily localised within the folded bilayer. The images in Fig. 8 indicate that *HPSE v2* colocalises with *HPSE v1* within the folded bilayer throughout gestation. Furthermore, *HPSE v2* signal intensity was significantly less than *HPSE v1* signal intensity, further suggesting that *HPSE v2* is a rare transcript variant.

Discussion

The pig placenta has one of the least invasive mammalian placentas (Dantzer *et al*. 1988; Leiser and Kaufmann 1994). As a result, the fetomaternal interface (i.e. the folded bilayer) of the pig placenta needs to increase in complexity and size as gestation progresses to allow for adequate fetomaternal exchange. The development and modification of the pig placenta is a complex biological process, which has not been characterised comprehensively. The results of the present study provide the first evidence that HPSE may play a role in modifying the fetomaternal interface of the pig placenta, especially during late gestation. In the present study, we report on the cloning of cDNAs encoding *HPSE*, the chromosomal location of *HPSE* and the mRNA expression pattern and localisation of *HPSE* in the pig placenta throughout gestation.

The cloning of *HPSE* from the pig placenta identified three transcript variants. The most abundant variant, *HPSE v1*, corresponded to a predicted full-length protein that shares 80% identity with human HPSE protein (Vlodavsky *et al*. 1999). The human *HPSE* gene is translated to a pre-pro HPSE protein that contains many regulatory elements (i.e. an N-terminal signal peptide, 8 and 50 kDa subunits, Cys residues, N-linked glycosylation sites and two catalytic residues) that are necessary for proper function (Vreys and David 2007). Many of these elements are conserved between the predicted pig protein for *HPSE v1* and the human HPSE protein. For instance, the N-terminal signal peptide and the sequence corresponding to the 8- and 50-kDa dimers that non-covalently bind for HPSE to become active are conserved between the pig and human HPSE protein. In addition, the predicted protein for *HPSE v1* contained all five Cys residues as well as four of the six N-linked glycosylation sites identified in the human protein (Vlodavsky *et al*. 1999; Vreys and David 2007). Furthermore, the two critical catalytic residues necessary for the hydrolysis of HS chains, a proton donor at Glu^{225} and a nucleophile at Glu^{343} (Hulett *et al*. 2000; Vreys and David 2007) were conserved in the predicted pig protein for *HPSE v1*. Because the predicted pig HPSE protein maintained conservation with many human HPSE functional domains, it is likely that the pig placenta produces a functional HPSE protein. Unfortunately, our initial attempts to identify HPSE protein in the pig placenta via western blot using several different commercial antibodies generated against human HPSE have been unsuccessful (J. L. Vallet, J. R. Miles, B. A. Freking, unpubl. obs.). However, follow-up investigations are ongoing to identify or produce a validated antibody for pig HPSE protein.

The two rare variants, namely *HPSE v2* and *v3*, identified in the pig placenta corresponded to predicted truncated proteins that appear to arise via alternative splicing. Alternatively spliced transcript variants for *HPSE* have been identified previously in the mole rat (Nasser *et al*. 2005) and human (Nasser *et al*. 2007; Sato *et al*. 2008). Alternative splicing of mRNA occurs via post-transcriptional modifications of a single transcript resulting in the generation of multiple mRNA precursors, which give rise to functionally different proteins (Kim *et al*. 2008). Alternative splicing typically occurs via four modifications: (*1*) exon skipping; (*2*) alternative 5′ splice sites; (*3*) alternative 3′ splice sites; and (*4*) intron retention (Kim *et al*. 2008). The additional 5′ sequence of *HPSE v2* in the pig placenta appears to have arisen from intron 2 retention, which incorporates several stop codons, resulting in a truncated protein of 81 amino acids. Although the function and identity of the predicted truncated protein corresponding to *HPSE v2* have yet to be determined, it is possible that this isoform may serve as an alternative isoform of the 8-kDa subunit identified in the human that forms a heterodimer with the larger 50-kDa subunit in the active protein (Vreys and David 2007). Therefore, it is possible that the truncated protein corresponding to *HPSE v2* may enhance or repress HPSE activity by serving as an alternative isoform of the 8-kDa protein.

The deleted 3′ sequence of both *HPSE v2* and *v3* appears to result from exon skipping of all of exons 9 and 10 and part of exon 8, which may have been removed via alternative 5′ and 3′ splice sites. The deleted 222 bp sequence in *HPSE v3* corresponded to a predicted truncated protein of 468 amino acids lacking 74 C-terminal amino acids. As a result, the predicted protein corresponding to *HPSE v3* lacks one of the two critical residues necessary for the hydrolysis of HS chains, the nucleophile at Glu^{343} (Vreys and David 2007). In the human, site-directed mutagenesis of either Glu^{225} or Glu^{343} in COS-7 cells resulted in complete abolishment of heparanase activity compared with the activity of wild-type HPSE or mutants for either Glu^{378} or Glu^{396} (Hulett *et al*. 2000). Furthermore, the splice 5 variant reported in the human kidney (Nasser *et al*. 2007) and placenta (Sato *et al*. 2008) resulted from skipping exon 5, which includes the proton donor at Glu^{225}. As a result, the transfection of human *HPSE* splice 5 variant into cells resulted in the elimination of heparanase activity compared with transfection of wild-type HPSE (Nasser *et al*. 2007; Sato *et al*. 2008). Therefore, the deletion of the critical residue at Glu^{343} in the predicted protein corresponding to *HPSE v3* identified in the pig placenta likely renders this isoform incapable of cleaving HS, thereby suggesting an inhibitory role of this variant on the action of HPSE in the pig placenta.

Several QTL for female reproductive traits have been identified on SSC8 (Rohrer *et al*. 1999; King *et al*. 2003). A QTL for uterine capacity has been identified at the 71 cM position on SSC8 (Rohrer *et al*. 1999). In addition, QTLs for litter size and prenatal survival have been identified at positions 127 and 125 cM on SSC8, respectively (King *et al*. 2003). The radiation hybrid mapping of the pig *HPSE* gene demonstrated that the pig *HPSE* gene is located between 126.1 and 127.7 cM on SSC8

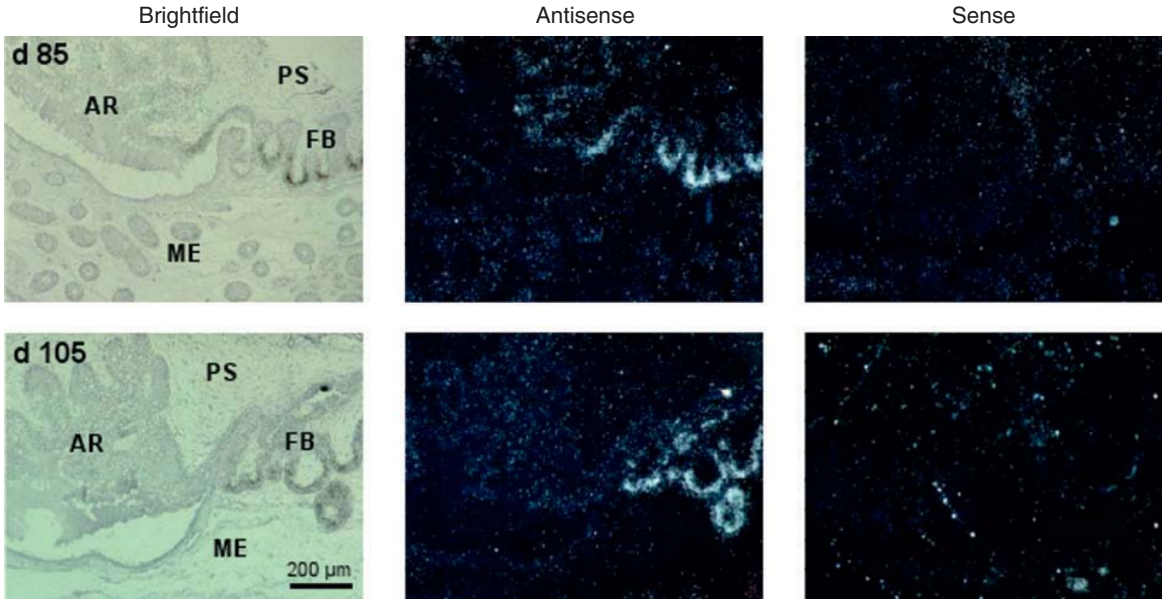

Fig. 7. *In situ* hybridisation analysis of *HPSE v1* mRNA localised to the fetomaternal interface of the pig placenta at Days 85 and 105 of gestation. Corresponding brightfield and darkfield with antisense probe or darkfield with sense probe photomicrographs are represented in uterine/placental cross-sections at Days 85 and 105 of gestation. These photomicrographs highlight that the *HPSE v1* signal is localised to the trophectoderm of the folded bilayer (FB), but is lacking in the placental areoli (AR) at the fetomaternal interface. In addition, the *HPSE v1* signal is lacking in cells of the maternal endometrium (ME) or placental stroma (PS). Scale bar = 200 μm.

based on the proximity of the *HPSE* gene to markers CL390254 and CL414431. Furthermore, comparative analysis of the pig *HPSE* gene with the human *HPSE* gene using the integrated radiation hybrid and linkage map (Meyers *et al*. 2005) demonstrated that the location of the pig *HPSE* corresponds to the location of human *HPSE* at 84.43 Mb on HSA4. The mapping of the pig *HPSE* gene to the distal portion of SSC8, in contrast with the central location of the human *HPSE* gene on HSA4, corroborates previous reports of an inversion of gene order between 80 and 150 Mb on HSA4, which corresponds to the map position of 70 cM to the distal end of SSC8 (Rohrer 1999; Kim *et al*. 2004; Meyers *et al*. 2005). As a result, the chromosomal location of the pig *HPSE* gene at the approximately 126 cM position is not in the region of the previously identified QTL for uterine capacity at the 71 cM position on SSC8 (Rohrer *et al*. 1999). However, the pig *HPSE* gene is in close proximity to the QTLs for litter size and prenatal survival, thereby indicating that *HPSE* is a good candidate gene for litter size and prenatal survival. We are presently attempting to identify polymorphisms within the pig *HPSE* gene that may be associated with litter size or prenatal survival.

Quantitative real-time PCR after reverse transcription is an extremely sensitive technique for measuring the amount of mRNA in biological samples. Two commonly used strategies for analysing real-time PCR data include absolute and relative quantification (Livak and Schmittgen 2001). For absolute quantification, the level of target mRNA is determined based on input copy numbers using a calibration curve of known amounts of starting material (Pfaffl 2004). In contrast, relative quantification determines the level of target mRNA relative to some reference control mRNA, usually an endogenous housekeeping gene such a *GAPDH* or *ACTB* (Pfaffl 2004). For proper analysis of data using relative quantification, it is imperative that the reference control mRNA be expressed at a constant level among samples and should be unaffected by the experimental treatment (Bustin 2000). Previous studies have demonstrated that *GAPDH* (Kuijk *et al*. 2007), *ACTB* (Miles *et al*. 2008*a*), *YWHAG* (Whitworth *et al*. 2005), *RPLP2* (Miles *et al*. 2008*b*) and *18S* (Kuijk *et al*. 2007) are stable endogenous controls in other porcine tissues. However, in the present study, the expression levels of these five putative internal control transcripts differed in the pig placenta according to day of gestation, as well as according to fetal littermate size. For all putative transcripts analysed, the greatest expression was observed in placental tissue at Day 25 of gestation compared with late gestation at Days 85 and 105. This suggests that placental tissue during early gestation has greater gene expression for these transcripts than compared with later stages of gestation, possibly through increased transcriptional activity or, alternatively, decreased mRNA turnover (degradation) from early stage placental tissue. A similar observation in the expression of *GAPDH* was reported between first- and third-trimester human placenta, in which *GAPDH* expression was greater in early gestation compared with late gestation and likely reflects differences in proliferative and developmental state of first-trimester human placentas (Patel *et al*. 2002). From the morphometric observations in the present study, as well as in

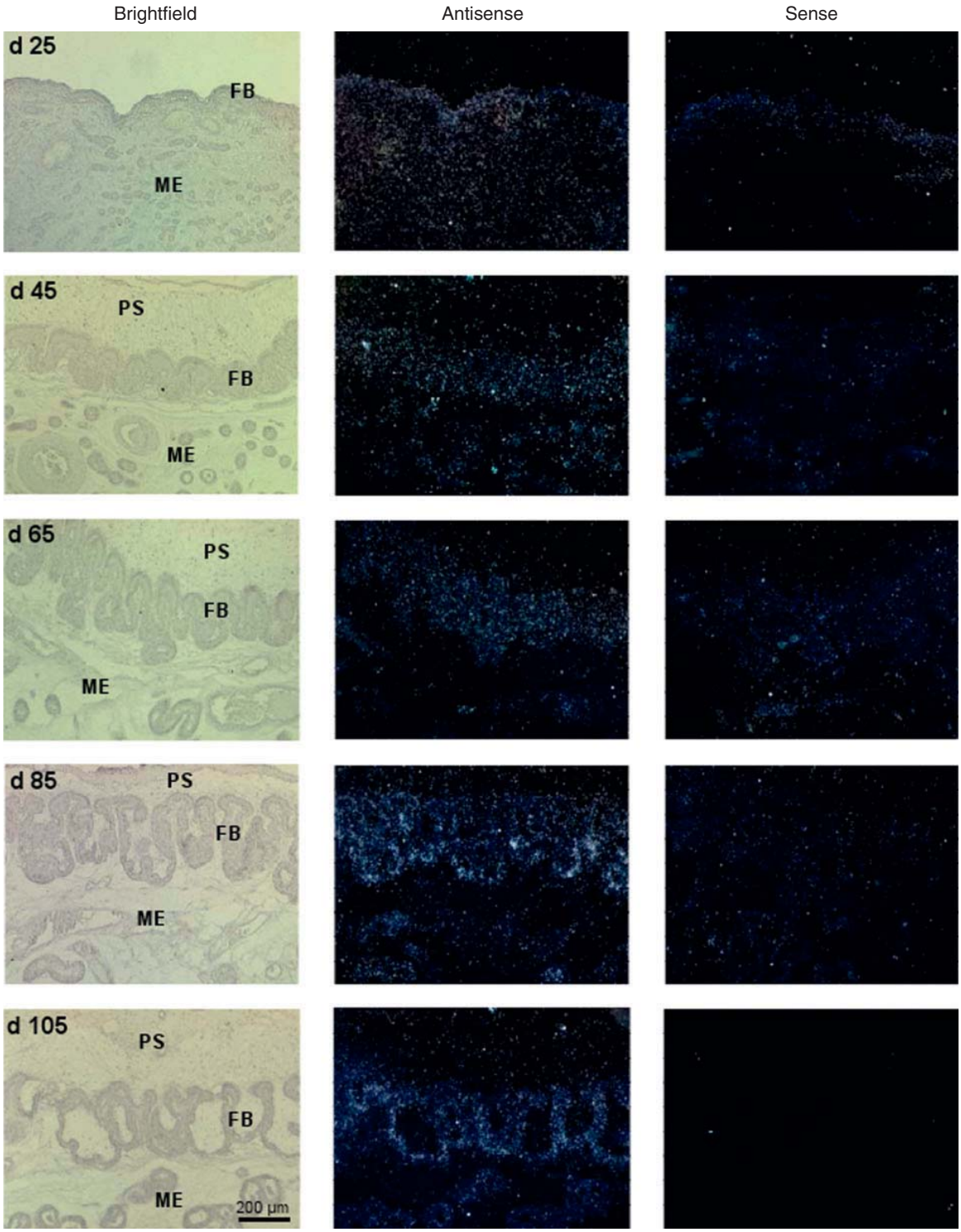

Fig. 8. *In situ* hybridisation analysis of *HPSE v2* mRNA localised to the fetomaternal interface of the pig placenta throughout gestation. Corresponding brightfield and darkfield with antisense probe or darkfield with sense probe photomicrographs are represented from uterine/placental cross-sections at Days 25, 45, 65, 85 and 105 of gestation. Note that throughout gestation the *HPSE v2* signal is localised to the trophectoderm of the folded bilayer (FB) and is lacking in cells of the maternal endometrium (ME) or placental stroma (PS). Scale bar = 200 μm.

earlier studies (Dantzer 1984; Vallet and Freking 2007), the morphology of the pig placenta is markedly different between early and late stages of gestation in the pig. Therefore, it is likely that gene(s) that regulate key biological functions differ markedly between these stages of gestation in the pig placenta. Because there were differences in the expression levels of these putative internal controls, the use of these transcripts to normalise gene expression of target genes for relative expression would be inappropriate. As a result, an absolute standard curve method (Pfaffl 2004) was used to determine the level of *HPSE v1* and *v2* mRNA in pig placenta.

The morphometric observations of the present study support previous reports (Dantzer 1984; Dantzer and Leiser 1994; Vallet and Freking 2007) demonstrating only minimal, irregular folding of the fetomaternal interface during early placentation (Day 25 of gestation), more regular but still thinner folded bilayer by mid-gestation (Days 45–65 of gestation), and greater complexity and width of the folded bilayer by late gestation (Days 85–105 of gestation). Although the exact mechanisms that regulate remodelling of the folded bilayer of the pig placenta are not known, recent evidence in mouse (D'Souza *et al*. 2007), baboon (D'Souza *et al*. 2008) and cow (Kizaki *et al*. 2003) suggests that modification of the basement membrane via breakdown of the HS by HPSE may result in the remodelling of the placenta during pregnancy. In the present study, real-time PCR analysis demonstrated elevated levels of expression for *HPSE v1* mRNA in placentas at Day 25 of gestation. Furthermore, ISH illustrated that the signal for *HPSE v1* in placentas at Day 25 of gestation was predominantly localised to the trophectoderm attached to uterine epithelium. At Day 15 of the cycle and pregnancy, HS was localised primarily to the basal lamina of the luminal epithelium in the pig (Cencic *et al*. 2003). Given the localisation of *HPSE* mRNA in the trophectoderm and HS in the uterine basement membrane during early gestation, it is possible that HPSE may play a role in early placentation by initiating the breakdown of HS in the basal lamina of the trophoblast and luminal epithelium, thereby preparing the basement membranes of the trophoblast epithelium and uterine endometrium to allow for the initiation of the folding in the bilayer.

After the initial folds of the bilayer have established during mid-gestation between Days 45 and 65, real-time PCR and ISH analysis demonstrated a downregulation of *HPSE v1* mRNA in the pig placenta, suggesting minimal activity of HPSE during mid-gestation. However, by late gestation, between Days 85 and 105, there was a resurgence of *HPSE v1* mRNA expression in the pig placenta, as illustrated by real-time PCR and ISH analysis, suggesting increased activity of HPSE during late gestation. During gestation in the pig, HS has been shown to decrease in placental homogenates as pregnancy progresses, with the lowest amounts of HS observed during late gestation (Steele and Froseth 1980). This illustrates that HS is actively degraded in the pig placenta as pregnancy progresses. Furthermore, this decrease in HS occurs in conjunction with changes in the morphology of the folded bilayer in which the folds become wider and more complex, indicating significant remodelling of the placenta (Dantzer 1984; Vallet and Freking 2007). Given the fact that only HPSE has been shown to actively break down HS (Vreys and David 2007; Nasser 2008), the increased expression of *HPSE v1* mRNA in conjunction with decreased HS during late gestation in the pig placenta homogenates suggests that HPSE likely results in a breakdown of HS in the pig placenta, which may result in modification of the placental architecture that occurs during this time.

Although the localisation of HS or HPSE protein in the pig placenta and maternal endometrium during late gestation have not been reported, the localisation of *HPSE v1* and *v2* mRNA in the present study was primarily confined to the trophectoderm along the walls of the folded bilayer nearest the endometrium, and this was especially apparent during late gestation. This suggests that HPSE activity is restricted to the basement membrane associated with the folded bilayer and it is likely that the majority of the HPSE activity is directed towards trophoblast basement membrane nearest to the maternal endometrium. Our initial hypothesis was that differences in *HPSE* mRNA expression would be observed between smallest and largest fetal pig littermates as a potential mechanism to account for previously reported differences in the morphology of the folded bilayer and placental stroma (i.e. increased folded bilayer widths with decreased placental stroma in the smallest littermates compared with the largest littermates; Vallet and Freking 2007). However, real-time PCR analysis for both *HPSE v1* and *v2* mRNA did not demonstrate significant fetal size effects. When separating trophectoderm from the uterine endometrium, portions of the trophoblast epithelium within the folds have been reported previously to remain adhered to the uterine epithelium, especially during late gestation (Dantzer 1984). Because the majority of the *HPSE* mRNA signal detected by ISH was primarily in the depths of the folds nearest the uterine epithelium, as well as along the walls of the folds, the lack of differences in *HPSE* mRNA expression between small and large littermates by real-time PCR could be explained by incomplete separation of the trophectoderm and uterine epithelium. Therefore, it is possible that HPSE activity may be greater in placentas from the smallest littermates given the facts that *HPSE* mRNA is localised primarily to the trophoblast cells nearest the uterine endometrium and that the smallest littermates have wider folds (Vallet and Freking 2007).

From the ISH of *HPSE v1*, it is clear that *HPSE v1* signal intensity is significantly greater during late gestation (Days 85 and 105) compared with early gestation (Day 25). However, real-time PCR analysis of *HPSE v1* demonstrated that the greatest level of expression was observed in placentas during early gestation (Day 25). Again, incomplete separation of trophectoderm and uterine endometrium during late gestation may explain the discrepancy in the level of expression observed by real-time PCR and signal intensity observed by ISH for *HPSE v1* observed during early gestation. Alternatively, placental tissue during early gestation may be more transcriptionally active compared with later stages of gestation, in which more mRNA is transcribed per μg total RNA. Increased transcriptional activity of early stage placental tissues is supported by the expression pattern observed for the putative housekeeping genes in the present study and a previous report in the human placenta (Patel *et al*. 2002).

We also anticipated greater remodelling at the tops of the folds towards the placental stroma given the observation that the width of the placental stroma above the folded bilayer decreases as pregnancy progresses and is significantly less in small littermate

placentas compared with large littermate placentas (Vallet and Freking 2007). However, based on the localisation of *HPSE* mRNA predominantly in trophoblast cells nearest the maternal endometrium in the present study, it appears that remodelling of the fetomaternal interface via HPSE likely involves remodelling of the trophoblast layer nearest the endometrium rather than the placental stroma. This is not to say that other mechanisms may play a role in the remodelling of the placental side of the fetomaternal interface. For instance, we have recently characterised the expression and activity of hyaluronidases, the enzymes that break down hyaluronan, in the pig placenta throughout gestation (J. L. Vallet, J. R. Miles, B. A. Freking, unpubl. obs.). This work indicated that hyaluronan is a key component of placental stroma and that hyaluronidases likely play a role in the restructuring of the stromal component of the placenta (J. L. Vallet, J. R. Miles, B. A. Freking, unpubl. obs.). These observations demonstrate the complexity of the development of the pig placenta, suggesting that a multitude of mechanisms potentially act on different components.

Real-time PCR and ISH analysis of *HPSE v2* mRNA illustrated that this transcript variant is a rarer variant than *HPSE v1* mRNA. This is consistent with the cDNA screening results from positive clones for HPSE indicating that *HPSE v1* was a more abundant transcript variant compared with *HPSE v2*. The expression pattern observed by real-time PCR for *HPSE v2* mRNA follows a similar pattern to that observed for *HPSE v1* mRNA (i.e. greater expression of *HPSE v2* on Days 85 and 105). Furthermore, ISH of *HPSE v2* illustrated a similar pattern of localisation, indicating colocalisation with *HPSE v1* in the trophectoderm within the folded bilayer. Taken together, these results suggest that *HPSE v2* may also play a role in modifying the fetomaternal interface in the pig. Whether the truncated form of HPSE corresponding to *HPSE v2* is translated and its possible role during pregnancy remain to be determined.

In summary, the cloning of cDNA from pig placenta identified three transcript variants similar to human HPSE. The abundant variant identified, namely *HPSE v1*, corresponded to a full-length protein that was highly conserved with the human HPSE protein, suggesting that the pig placenta produces a functional HPSE protein. The chromosomal location of the pig *HPSE* gene was mapped in close proximity to QTLs for litter size and prenatal survival on SSC8, suggesting that genetic variation in the *HPSE* gene could be associated with litter size and prenatal survival. In addition, the expression level of *HPSE v1* mRNA was elevated in placentas during early placentation (Day 25), as well as during late gestation (Days 85 and 105). Furthermore, *HPSE v1* mRNA was primarily expressed in the trophectoderm of the folded bilayer throughout gestation. During late gestation, the localisation of *HPSE* mRNA was primarily along the folded bilayer wall, with significant localisation in trophoblast epithelial cells nearest the uterine endometrium. These observations suggest that HPSE may play a role in the folding of the fetomaternal interface during early gestation and that HPSE may play a role in modifying the fetomaternal interface during late gestation. Taken together, the results of the present study suggest that HPSE plays a role in the development of the pig placenta, which may have implications for litter size, prenatal survival and postnatal piglet health. Follow-up investigations are ongoing to better understand the regulation of HPSE in the development of the pig placenta, particularly focusing on the identification of the HPSE protein in regards to the location of HS, as well as the level of HPSE activity, within various components of the pig placenta.

Acknowledgements

The authors thank Susan Hassler and Troy Gramke for technical assistance in the collection and processing of samples, David Sypherd for assistance with *in situ* hybridisation, Alan Kruger for assistance with microscopy, Susan Hauver for assistance with radiation hybrid mapping, the USMARC swine crew for animal husbandry, the USMARC abattoir crew for assistance with killing of the pigs and Drs David Guthrie (US Department of Agriculture – Agricultural Research Service, Beltsville Agricultural Research Center) and Leah Zorrilla (US Environmental Protection Agency, National Health and Environmental Effects Research Laboratory) for critical review of this manuscript. This research was supported by USDA-ARS, CRIS Project No. 5438–31000–084–00D.

References

Bustin, S. A. (2000). Absolute quantification of mRNA using real-time reverse transcription polymerase chain reaction assays. *J. Mol. Endocrinol.* **25**, 169–193. doi:10.1677/JME.0.0250169

Cencic, A., Guillomot, M., Koren, S., and La Bonnardiere, C. (2003). Trophoblastic interferons: do they modulate uterine cellular markers at the time of conceptus attachment in the pig? *Placenta* **24**, 862–869. doi:10.1016/S0143-4004(03)00135-8

Christenson, R. K., Leymaster, K. A., and Young, L. D. (1987). Justification of unilateral hysterectomy–ovariectomy as a model to evaluate uterine capacity in swine. *J. Anim. Sci.* **65**, 738–744.

Dantzer, V. (1984). Scanning electron microscopy of exposed surfaces of the porcine placenta. *Acta Anat.* **118**, 96–106. doi:10.1159/000145827

Dantzer, V., and Leiser, R. (1994). Initial vascularisation in the pig placenta: I. Demonstration of nonglandular areas by histology and corrosion casts. *Anat. Rec.* **238**, 177–190. doi:10.1002/AR.1092380204

Dantzer, V., Leiser, R., Kaufmann, P., and Luckhardt, M. (1988). Comparative morphological aspects of placental vascularization. *Trophoblast Res.* **3**, 235–260.

Dong, J., Kukula, A. K., Toyoshima, M., and Nakajima, M. (2000). Genomic organization and chromosome localization of the newly identified human heparanase gene. *Gene* **253**, 171–178. doi:10.1016/S0378-1119(00)00251-1

D'Souza, S. S., Daikoku, T., Farach-Carson, M. C., and Carson, D. D. (2007). Heparanase expression and function during early pregnancy in mice. *Biol. Reprod.* **77**, 433–441. doi:10.1095/BIOLREPROD.107.061317

D'Souza, S. S., Fazleabas, A. T., Banerjee, P., Sherwin, J. R., Sharkey, A. M., Farach-Carson, M. C., and Carson, D. D. (2008). Decidual heparanase activity is increased during pregnancy in the baboon (*Papio anubis*) and in *in vitro* decidualization of human stromal cells. *Biol. Reprod.* **78**, 316–323. doi:10.1095/BIOLREPROD.107.063891

Freking, B. A., Leymaster, K. A., Vallet, J. L., and Christenson, R. K. (2007). Number of fetuses and conceptus growth throughout gestation in lines of pigs selected for ovulation rate or uterine capacity. *J. Anim. Sci.* **85**, 2093–2103. doi:10.2527/JAS.2006-766

Hashizume, K. (2007). Analysis of uteroplacental-specific molecules and their functions during implantation and placentation in the bovine. *J. Reprod. Dev.* **53**, 1–11. doi:10.1262/JRD.18123

Hulett, M. D., Hornby, J. R., Ohms, S. J., Zuegg, J., Freeman, C., Gready, J. E., and Parish, C. R. (2000). Identification of active-site residues of the pro-metastatic endoglycosidase heparanase. *Biochemistry* **39**, 15 659–15 667. doi:10.1021/BI002080P

Kim, E., Goren, A., and Ast, G. (2008). Alternative splicing: current perspectives. *Bioessays* **30**, 38–47. doi:10.1002/BIES.20692

Kim, J. G., Rohrer, G. A., Vallet, J. L., Christenson, R. K., and Nonneman, D. (2004). Addition of 14 anchored loci to the porcine chromosome 8 comparative map. *Anim. Genet.* **35**, 474–476. doi:10.1111/J.1365-2052.2004.01197.X

King, A. H., Jiang, Z., Gibson, J. P., Haley, C. S., and Archibald, A. L. (2003). Mapping quantitative trait loci affecting female reproductive traits on porcine chromosome 8. *Biol. Reprod.* **68**, 2172–2179. doi:10.1095/BIOLREPROD.102.012955

Kizaki, K., Yamada, O., Nakano, H., Takahashi, T., Yamauchi, N., Imai, K., and Hashizume, K. (2003). Cloning and localization of heparanase in bovine placenta. *Placenta* **24**, 424–430. doi:10.1053/PLAC.2002.0909

Kuijk, E. W., du Puy, L., van Tol, H. T., Haagsman, H. P., Colenbrander, B., and Roelen, B. A. (2007). Validation of reference genes for quantitative RT-PCR studies in porcine oocytes and preimplantation embryos. *BMC Dev. Biol.* **7**, 58. doi:10.1186/1471-213X-7-58

Leiser, R., and Kaufmann, P. (1994). Placental structure: in a comparative aspect. *Exp. Clin. Endocrinol.* **102**, 122–134.

Livak, K. J., and Schmittgen, T. D. (2001). Analysis of relative gene expression data using real-time quantitative PCR and the $2^{-\Delta\Delta Ct}$ method. *Methods* **25**, 402–408. doi:10.1006/METH.2001.1262

Meyers, S. N., Rogatcheva, M. B., Larkin, D. M., Yerle, M., Milan, D., Hawken, R. J., Schook, L. B., and Beever, J. E. (2005). Piggy-BACing the human genome II. A high-resolution, physically anchored, comparative map of the porcine autosomes. *Genomics* **86**, 739–752. doi:10.1016/J.YGENO.2005.04.010

Miles, J. R., Freking, B. A., Blomberg, L. A., Vallet, J. L., and Zuelke, K. A. (2008*a*). Conceptus development during blastocyst elongation in lines of pigs selected for increased uterine capacity or ovulation rate. *J. Anim. Sci.* **86**, 2126–2134. doi:10.2527/JAS.2008-1066

Miles, J. R., Blomberg, L. A., Krisher, R. L., Everts, R. E., Sonstegard, T. S., Van Tassell, C. P., and Zuelke, K. A. (2008*b*). Comparative transcriptome analysis of *in vivo*- and *in vitro*-produced porcine blastocysts by small amplified RNA–serial analysis of gene expression (SAR-SAGE). *Mol. Reprod. Dev.* **75**, 976–988. doi:10.1002/MRD.20844

Nasser, N. J. (2008). Heparanase involvement in physiology and disease. *Cell. Mol. Life Sci.* **65**, 1706–1715. doi:10.1007/S00018-008-7584-6

Nasser, N. J., Nevo, E., Shafat, I., Ilan, N., Vlodavsky, I., and Avivi, A. (2005). Adaptive evolution of heparanase in hypoxia-tolerant Spalax: gene cloning and identification of a unique splice variant. *Proc. Natl Acad. Sci. USA* **102**, 15 161–15 166. doi:10.1073/PNAS.0507279102

Nasser, N. J., Avivi, A., Shushy, M., Vlodavsky, I., and Nevo, E. (2007). Cloning, expression, and characterization of an alternatively spliced variant of human heparanase. *Biochem. Biophys. Res. Commun.* **354**, 33–38. doi:10.1016/J.BBRC.2006.12.189

Patel, P., Boyd, C. A., Johnston, D. G., and Williamson, C. (2002). Analysis of GAPDH as a standard for gene expression quantification in human placenta. *Placenta* **23**, 697–698. doi:10.1053/PLAC.2002.0859

Patel, V. N., Knox, S. M., Likar, K. M., Lathrop, C. A., Hossain, R., Eftekhari, S., Whitelock, J. M., Elkin, M., Vlodavsky, I., and Hoffman, M. P. (2007). Heparanase cleavage of perlecan heparan sulfate modulates FGF10 activity during *ex vivo* submandibular gland branching morphogenesis. *Development* **134**, 4177–4186. doi:10.1242/DEV.011171

Pfaffl, M. W. (2001). A new mathematical model for relative quantification in real-time RT-PCR. *Nucleic Acids Res.* **29**, e45. doi:10.1093/NAR/29.9.E45

Pfaffl, M. W. (2004). Quantification strategies in real-time PCR. In 'A–Z of quantitative PCR'. (Ed. S. A. Bustin.) pp. 89–113. (International University Line: La Jolla.)

Regnault, T. R., Galan, H. L., Parker, T. A., and Anthony, R. V. (2002). Placental development in normal and compromised pregnancies: a review. *Placenta* **23**(Suppl. A), S119–S129. doi:10.1053/PLAC.2002.0792

Rohrer, G. A. (1999). Mapping four genes from human chromosome 4 to porcine chromosome 8 further develops the comparative map for an economically important chromosome of the swine genome. *Anim. Genet.* **30**, 60–63. doi:10.1046/J.1365-2052.1999.00421.X

Rohrer, G. A., Ford, J. J., Wise, T. H., Vallet, J. L., and Christenson, R. K. (1999). Identification of quantitative trait loci affecting female reproductive traits in a multigeneration Meishan-White composite swine population. *J. Anim. Sci.* **77**, 1385–1391.

Rozen, S., and Skaletsky, H. (2000). Primer3 on the WWW for general users and for biologist programmers. *Methods Mol. Biol.* **132**, 365–386.

SAS (2003). 'The SAS System for Windows, release 9.1.' (SAS Institute, Inc.: Cary, NC.)

Sato, M., Amemiya, K., Hayakawa, S., and Munakata, H. (2008). Subcellular localization of human heparanase and its alternative splice variant in COS-7 cells. *Cell Biochem. Funct.* **26**, 676–683. doi:10.1002/CBF.1492

Spencer, T. E., Ing, N. H., Ott, T. L., Mayes, J. S., Becker, W. C., Watson, G. H., Mirando, M. A., and Brazer, F. W. (1995). Intrauterine injection of ovine interferon-tau alters oestrogen receptor and oxytocin receptor expression in the endometrium of cyclic ewes. *J. Mol. Endocrinol.* **15**, 203–220. doi:10.1677/JME.0.0150203

Steel, R. G. D., Torrie, J. H., and Dickey, D. A. (1997). 'Principles and Procedures of Statistics: A Biometrical Approach.' (McGraw-Hill: New York.)

Steele, V. S., and Froseth, J. A. (1980). Effect of gestational age on the biochemical composition of porcine placental glycosaminoglycans. *Proc. Soc. Exp. Biol. Med.* **165**, 480–485.

Vallet, J. L., and Freking, B. A. (2007). Differences in placental structure during gestation associated with large and small pig fetuses. *J. Anim. Sci.* **85**, 3267–3275. doi:10.2527/JAS.2007-0368

Vlodavsky, I., Friedmann, Y., Elkin, M., Aingorn, H., Atzmon, R., *et al*. (1999). Mammalian heparanase: gene cloning, expression and function in tumor progression and metastasis. *Nat. Med.* **5**, 793–802. doi:10.1038/10518

Vlodavsky, I., Goldshmidt, O., Zcharia, E., Atzmon, R., Rangini-Guatta, Z., Elkin, M., Peretz, T., and Friedmann, Y. (2002). Mammalian heparanase: involvement in cancer metastasis, angiogenesis and normal development. *Semin. Cancer Biol.* **12**, 121–129. doi:10.1006/SCBI.2001.0420

Vreys, V., and David, G. (2007). Mammalian heparanase: what is the message? *J. Cell. Mol. Med.* **11**, 427–452. doi:10.1111/J.1582-4934.2007.00039.X

Whitworth, K. M., Agca, C., Kim, J.-G., Patel, R. V., Springer, G. K., Bivens, N., Forrester, L. J., Mathialagan, N., Green, J. A., and Prather, R. S. (2005). Transcriptional profiling of pig embryogenesis by using a 15-k member unigene set specific for pig reproductive tissues and embryos. *Biol. Reprod.* **72**, 1437–1451. doi:10.1095/BIOLREPROD.104.037952

Yerle, M., Pinton, P., Robica, A., Alfonsoa, A., Palvadeaua, Y., *et al*. (1998). Construction of a whole-genome radiation hybrid panel for high-resolution gene mapping in pigs. *Cytogenet. Cell Genet.* **82**, 182–188. doi:10.1159/000015095

Zcharia, E., Metzger, S., Chajek-Shaul, T., Aingorn, H., Elkin, M., Friedmann, Y., Weinstein, T., Li, J. P., Lindahl, U., and Vlodavsky, I. (2004). Transgenic expression of mammalian heparanase uncovers physiological functions of heparan sulfate in tissue morphogenesis, vascularization, and feeding behavior. *FASEB J.* **18**, 252–263. doi:10.1096/FJ.03-0572COM

Zhang, S., Bidanel, J. P., Burlot, T., Legault, C., and Naveau, J. (2000). Genetic parameters and genetic trends in the Chinese × European Tiameslan composite pig line. I. Genetic parameters. *Genet. Sel. Evol.* **32**, 41–56. doi:10.1051/GSE:2000105

Manuscript received 25 February 2009, accepted 10 May 2009